

Triplet Excited States and Radical Intermediates Formed in Electron Pulse Radiolysis of Amino and Dimethylamino Derivatives of Benzophenone

Ajay K. Singh, Dipak K. Palit,* and Tulsi Mukherjee

Radiation Chemistry & Chemical Dynamics Division, Bhabha Atomic Research Centre, Mumbai 400 085, India

Received: December 31, 2001; In Final Form: April 8, 2002

The electron pulse radiolysis technique has been used to study the spectral, kinetic, and radiation chemical properties of the triplet excited states as well as the reduced and oxidized radicals of 2-amino-, 4-amino-, 4-(dimethylamino)-, and 4,4'-bis(dimethylamino)benzophenones. Hydrated electron (e_{aq}^-) has been found to react with these benzophenone derivatives to form the anion radical species with the rate constants varying from $(4 \text{ to } 10) \times 10^9 \text{ dm}^3 \text{ mol}^{-1} \text{ s}^{-1}$, which are slower than that for the parent ketone, benzophenone. The spectral and kinetic properties of the transient ketyl and anion radicals have been studied by generating them at suitable pH. The absorption peaks of the ketyl radicals appear in the region 565–630 nm and those of the anion radicals are red shifted in the wavelength region 565–630 nm. The pK_a values of the ketyl \leftrightarrow anion radical equilibria vary from 8.8 to 10.7 for various substituted aminobenzophenones. The cation radicals of these derivatives have been generated by pulse radiolysis in 1,2-dichloroethane and tetrachloromethane solvents along with other transient species, such as ion pairs and radical adducts. The triplet states of these compounds have been generated in benzene. The probable mechanism of the self-quenching interaction between the triplet and the ground state is the simple hydrogen atom abstraction reaction by the $n\pi^*$ triplet, which is energetically close to the lower lying $\pi\pi^*$ triplet state. Mechanisms of interaction between the ground states of the amino-substituted benzophenone derivatives and the benzophenone triplet have been found to depend on the driving force for the charge- or electron-transfer reaction between the members of a particular pair. $n\pi^*$ Triplet state of benzophenone interacts with 2-aminobenzophenone via energy transfer to the latter, with 4-aminobenzophenone via hydrogen atom abstraction and with 4-(dimethylamino)- and 4,4'-bis(dimethylamino)-benzophenones by electron-transfer coupled with proton-transfer reactions. Only in the case of the interaction between triplet benzophenone and 4-(dimethylamino)benzophenone, evidence for exciplex formation has been obtained.

1. Introduction

The photochemistry of aromatic ketones, specially benzophenone (BP) and its derivatives, has been extensively studied because of their wide use as photosensitizers as well as electron and hydrogen atom acceptors.^{1,2} The lowest excited triplet (T_1) state, which is the initiator of these reactions, is capable of abstracting a hydrogen atom from a variety of substrates including aliphatic hydrocarbons, alcohols, phenols, and amines.^{1–10} One intriguing aspect of this well-studied photoreduction reaction undergone by the ketone triplet is the fact that it may occur either by direct transfer of a hydrogen atom from a donor molecule to its carbonyl group or by transfer of an electron from the donor to the ketone followed by transfer of a proton from the donor cation to the ketone radical anion thus formed (i.e., by coupled electron- and proton-transfer process). The ketyl radical is the transient produced in either of the two cases.^{4,11–13} Several attempts have been made to identify the structural features dictating the changeover from the atom-transfer to the electron-transfer mechanism in the photoreduction of carbonyl compounds. It is well established from various studies reported earlier that the rate, efficiency, and mechanism of this reaction depend on the nature and characteristics of the T_1 state of the carbonyl compound as well as the nature of the

hydrogen atom donor.^{1,4–6,14,15} Three kinds of triplet excited states, namely, $n\pi^*$, $\pi\pi^*$, and CT (the latter is in fact an unsymmetrically charge-distributed $\pi\pi^*$ state), have been identified as being responsible for the difference in their photophysical and photochemical reactivities.^{4,9,16} The nature of the T_1 state of an aromatic carbonyl compound depends on the nature of the substituent as well as the solvent.^{10,17,18}

A large number of studies have been reported on the reactivities of the $n\pi^*$ and $\pi\pi^*$ triplet states toward the hydrogen atom abstraction reaction. However, there is no fixed rule on the intrinsic ratio of the reactivities of $n\pi^*$ and $\pi\pi^*$ triplets.⁴ The reactivity and mechanism of the hydrogen atom abstraction reaction mainly depend on the thermodynamic feasibility or the change in free energy of the electron-transfer reaction (ΔG_{et}) from the donor to the T_1 state of the ketone. If the charge-transfer reaction is thermodynamically allowed (i.e., ΔG_{et} is negative), both the $n\pi^*$ and $\pi\pi^*$ triplets are equally reactive and the reaction possibly involves the formation of a charge-transfer (CT) type triplet exciplex. However, the reactivity of the $\pi\pi^*$ triplet is reduced with a decrease in the reduction potential of the triplet. In the latter case the extent of charge transfer in the CT complex is smaller and hydrogen atom transfer becomes the rate-determining step, dropping the reactivity of the $\pi\pi^*$ triplet. In case the electron-transfer interaction between the T_1 state of the ketone and the hydrogen atom donor is not thermodynamically favorable (i.e., ΔG_{et} is positive), the

* Author for correspondence. E-mail: dkpalit@apsara.barc.ernet.in. Fax: 91-22-550-5151.

mechanism of photoreduction resembles simple hydrogen atom abstraction and the reactivity of the $n\pi^*$ triplet is more than 10^3 times higher than that of $\pi\pi^*$ or CT triplet state.^{5,6,20–23} It has also been shown that the inductive effect of the substituents on rate constants for hydrogen atom abstraction by the $n\pi^*$ triplets is quite small.²⁴

In the case of BP, the parent of the aromatic carbonyl compounds, its T_1 state is produced with the quantum yield close to unity and is responsible for all the photochemical reactions undergone by this molecule.²⁵ The T_1 state of BP has been shown to have $n\pi^*$ configuration in all kinds of solvents and the higher energy $\pi\pi^*$ triplet state remains much above the $n\pi^*$ T_1 state in the energy level diagram.^{17,26} However, on substitution with electron donating groups such as OH, OCH₃, NH₂, and N(CH₃)₂ onto the aromatic rings of benzophenone, the relative position of $n\pi^*$ and $\pi\pi^*$ states are largely altered depending on the nature and position of the substituent and also by the solvent polarity.^{17,19,23,26} From the results of our recent flash photolysis studies as well as the studies reported earlier on hydroxy-, amino- and dimethylamino-substituted benzophenones, we could explore two important aspects of their reactivity.^{4,17,19,23,26} First, in nonpolar solvents, such as cyclohexane and benzene, the positions of the $n\pi^*$ and $\pi\pi^*$ T_1 states lie very close to each other and the triplet levels are interconverted, forming an equilibrium under thermal activation. Hence the reactivity of the T_1 states of these molecules toward hydrogen atom abstraction in these solvents are retained due to the presence of the $n\pi^*$ state in equilibrium with the $\pi\pi^*$ one. However, the equilibrium constant for the triplet level interconversion becomes part of the reduced reactivity of their triplet state.^{18a} In polar solvents the T_1 state is a $\pi\pi^*$ or CT state and the intersystem-crossing yield is also lower. Hence, both the reactivity and the product yield are considerably reduced for these benzophenone derivatives as compared to those of the parent. Second, the electron donation by the amino and dimethylamino groups could reduce the electrophilicity at the oxygen atom and hence the rates as well as the efficiency of the hydrogen atom abstraction reaction are reduced.

Despite the reduced reactivities of amino- and dimethylamino-substituted benzophenones (compared to that of BP) towards hydrogen atom abstraction reactions from the solvent molecules, such as cyclohexane, the T_1 states of these ketone derivatives have been seen to be efficiently quenched by their ground states.^{24,26} The relatively large values of self-quenching rate constants for 4,4'-bis(dimethylamino)benzophenone or Michler's ketone (MK) in nonpolar solvents (10^7 to 10^8 dm³ mol⁻¹ s⁻¹),^{26,27,28} as compared with the values of $\sim 10^5$ dm³ mol⁻¹ s⁻¹ for benzophenone ($n\pi^*$ triplet)^{28,29} and methyl-2-naphthyl ketone ($\pi\pi^*$ triplet),³⁰ suggest that the self-quenching interaction in MK is highly favorable, probably due to charge-transfer interaction. Many authors have suggested the possibility of formation of triplet excimer as an intermediate to explain the mechanism of such an efficient self-quenching reaction.^{26,31} However, efforts to characterize the triplet excimers in these systems have been fruitless.

In the present study, we have made an attempt to characterize the spectroscopic and kinetic properties of various radical species of amino- and dimethylamino-substituted derivatives of benzophenone using the electron pulse radiolysis absorption spectroscopic technique. Benzophenone and its derivatives have high reactivities toward hydrated electron producing ketyl or anion radicals with good yield. A radical anion, generated directly through the hydrated electron reaction, is protonated to form the ketyl radical at a suitable pH. The advantage of

this technique over that of flash photolysis is that it does not involve the triplet state in the generation of the ketyl radical. The pulse radiolysis technique also provides convenient mechanisms of generating the cation radicals and the triplet states (see later). Generation of the latter does not involve the singlet state as the precursor and hence its yield is not dependent on the intersystem-crossing yield. Hence this technique provides us the convenience of investigating the interaction between the T_1 state of BP and the ground state of its amino derivatives in order to correlate the mechanism of the reaction with their reduction potentials.

2. Experimental Section

The amino derivatives of benzophenone, namely, 2-(or *ortho*-)aminobenzophenone (OABP) and 4-(or *para*-)aminobenzophenone (PABP) and the dimethylamino derivatives, namely, 4-(dimethylamino)benzophenone (DMABP) and 4,4'-bis(dimethylamino)benzophenone (MK), were obtained from Aldrich. PABP was purified by repeated crystallization from an aqueous-ethanol mixture. OABP, DMABP, or MK was recrystallized from methanol. Solvents used were of spectroscopic grade (Spectrochem) and used without further purification. High-purity nitrogen gas (Indian Oxygen, purity >99.9%) was used to deaerate the samples. All experiments were carried out at room temperature (298 ± 1 K) unless specified otherwise. Buffer solutions were prepared from the suitable mixtures of solutions of Na₂HPO₄ and NaH₂PO₄. Aqueous solutions were prepared in nano-pure water obtained from a Barnstead System (resistivity 18.3 MΩ cm). The oxidation potentials of the amino-substituted benzophenones were determined in acetonitrile solution using tetrafluoroborate salt as the supporting electrolyte by using Ag/Ag⁺ electrode as the reference electrode with an Autolab model AUT 70909 cyclic voltammeter.

Detailed experimental set-up for the electron pulse radiolysis and the kinetic absorption spectrophotometric technique used here has been described elsewhere.³² Sample solutions taken in a suprasil cuvette of 1 cm path length were irradiated by electron pulses of 50 ns duration (fwhm) from a 7 MeV linear electron accelerator (Forward Industries) at a radiation dose of 10–12 Gy per pulse as measured by an air saturated 0.05 mol dm⁻³ KSCN dosimeter, taking $G\epsilon$ for (SCN)₂ as 21 522 dm³ mol⁻¹ cm⁻¹ at 500 nm (G being defined as number of molecules formed per 100 eV energy absorbed).³³ The transient absorption profiles were monitored by a kinetic absorption spectrophotometric arrangement consisting of a 450 W pulsed xenon lamp in conjunction with a monochromator (Kratos Model 152A) and photo-multiplier tube (Hamamatsu R-928), connected to a digital oscilloscope (L&T Gould 4072). The data were transferred to an IBM-PC where data analysis was carried out with indigenously developed program.

3. Results and Discussion

(a) **Reaction of e_{aq}^- .** Electron pulse radiolysis of water generates three major primary reactive species, e_{aq}^- , $\cdot\text{OH}$, and H^\cdot with G values 2.7, 2.7, and 0.5, respectively. The G value for e_{aq}^- is constant (2.7) in the pH range 4–10.³⁴ Although no data are being reported here for pH < 4, a few experiments have been performed in solutions with pH > 10, at which $G(e_{aq}^-)$ is greater than 2.7 and in such cases the actual values of $G(e_{aq}^-)$ reported at the respective pH's have been used.³⁴ Among the three primary species, $\cdot\text{OH}$ is the oxidizing species while the other two are reducing in nature. By adding suitable scavengers in the solution, the reaction conditions could be

TABLE 1: Spectroscopic and Kinetic Characteristics of the Ketyl and Anion Radical Species of ABP's

compound	$k_{e_{aq}^-}$, $\text{dm}^3 \text{mol}^{-1} \text{s}^{-1}$	ketyl radical				pK_a	anion radical		
		λ_{max} , nm	ϵ , $\text{dm}^3 \text{mol}^{-1} \text{cm}^{-1}$	$2k$, $\text{dm}^3 \text{mol}^{-1} \text{s}^{-1}$	λ_{max} , nm		ϵ , $\text{dm}^3 \text{mol}^{-1} \text{cm}^{-1}$	$2k$, $\text{dm}^3 \text{mol}^{-1} \text{s}^{-1}$	
OABP	4.4×10^9	540	1800	1.4×10^9	8.8	565	4000	5.6×10^8	
PABP	1×10^{10}	550	2300	1.3×10^9	9.8	600	5200	4×10^8	
DMABP	9.8×10^9	550	2460	9.6×10^8	10.2	610	5700	3.8×10^8	
MK	8×10^9	580	1700	3.9×10^8	10.7	630	4500	3×10^8	

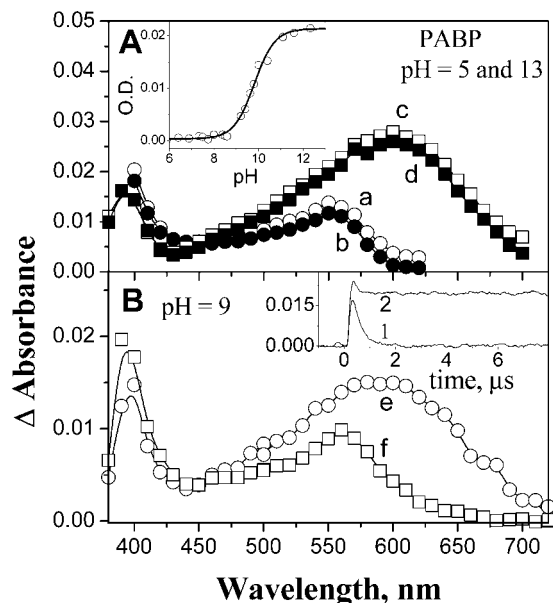
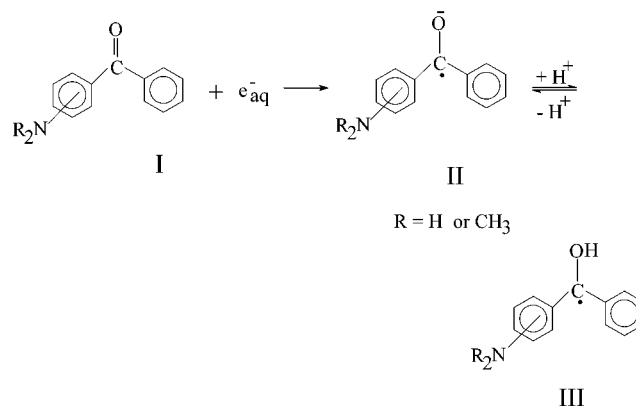


Figure 1. Time-resolved absorption spectra of the transient radical species produced due to reaction of e_{aq}^- with PABP in aqueous solutions at pH 5 (spectra a and b), 13 (spectra c and d), and 9 (spectra e and f). They are recorded at 0.8 μs (spectra a, c, and e) and 20 μs (spectra b, d, and f), respectively, after the electron pulse. Inset of A shows the absorbance changes recorded at 620 nm as a function of pH due to reaction of e_{aq}^- with PABP. The line represents the fit function to follow the eq i. The pK_a value thus obtained is given in Table 1. Inset of B shows the kinetic traces recorded at 720 nm due to pulse radiolysis of solutions at pH 5 (curve 1) and 13 (curve 2), respectively. Spectra a, b, and f have been assigned to the ketyl radical of PABP (structure III), and c–e, to the anion radical of PABP (structure II).

adjusted in such a way that only the reaction of e_{aq}^- with the solutes could be exclusively studied. The kinetics of the reaction of e_{aq}^- with the amino derivatives of benzophenone (abbreviated as ABP) have been studied in deaerated aqueous solutions containing $\sim 1 \text{ mol dm}^{-3}$ *tert*-butyl alcohol and different concentrations (2.5×10^{-5} to $2 \times 10^{-3} \text{ mol dm}^{-3}$) of the ABP's. *tert*-Butyl alcohol scavenges the oxidizing $\cdot\text{OH}$ radical efficiently and also increases the solubility of the ABP's in aqueous solutions. The decay kinetics of e_{aq}^- at different pH conditions have been monitored at 720 nm and the second-order rate constant values ($k_{e_{aq}^-}$) were evaluated from the slope of the linear plot of the e_{aq}^- pseudo-first-order rate constants vs the concentrations of ABP (Table 1). The rate constant values are much smaller than that reported for BP ($2.8 \times 10^{10} \text{ dm}^3 \text{mol}^{-1} \text{s}^{-1}$)^{35,36} in aqueous solutions. Considering the fact that $>\text{C}=\text{O}$ group is the most electron affinic center in the ABP molecule, the electron is evidently captured by the molecule at this center to produce the anion radical species as the primary reaction product. Hence, the rate constants for the reaction between e_{aq}^- and ABP's are seen to decrease in the same order (Table 1) as the increase in electron-donating ability ($2\text{N}(\text{CH}_3)_2 > \text{N}(\text{CH}_3)_2 > \text{NH}_2$) of the substituent groups. The smaller value of the rate constant for OABP than that for PABP is evidently due to the presence of an intramolecular hydrogen bond in the former.

SCHEME 1

The time-resolved spectra recorded soon after the electron decay (i.e., at 0.8 μs) and at 20 μs after the electron pulse and the decay kinetics of the transient radical species produced due to the reaction of e_{aq}^- with PABP ($1 \times 10^{-3} \text{ mol dm}^{-3}$) in aqueous solutions of three different pH's have been presented in Figure 1. At this concentration of PABP, the reaction with e_{aq}^- is complete within 0.8 μs , as seen from the decay of the hydrated electron monitored at 720 nm. This is evident from the nature of traces 1 and 2 in the inset of Figure 1B. Hence the spectra of the transient radical species being reported here have been recorded at or later than 0.8 μs after the electron pulse reaching the sample. Figure 1A shows that the natures of the transient radical spectra at pH 5 and 13 are quite different, having peaks at 550 and 600 nm, respectively. In both the cases the transient spectra do not evolve in the 0.8–20 μs time domain. However, the transient absorption spectrum recorded at 0.8 μs after the electron pulse irradiation of a solution buffered at pH 9 (spectrum e in Figure 1B) shows a peak at ca. 600 nm, and it is similar to that obtained at pH 13 (spectra c and d). The transient absorption in 570–700 nm region decays faster, and spectrum f, recorded at 20 μs , is very similar to that obtained at pH 5 (spectra a and b). Spectrum e, recorded at 0.8 μs , could be attributed to the radical anion (II) formed due to electron attachment to PABP (I) and the ketyl radical (III), which has subsequently been formed due to protonation of the precursor anion radical (II) (Scheme 1). The wavelength maxima (λ_{max}) of the ketyl and anion radical spectra of ABP's, generated by reaction with e_{aq}^- in solutions of pH 5 and 13, respectively, the molar extinction coefficient (ϵ), and the second-order decay rate constant ($2k$) values calculated for these radical species have been presented in Table 1.

To obtain the pK_a values for the acid–base equilibrium for the ketyl radical–radical anion conversion process (i.e., $\text{II} \rightleftharpoons \text{III}$), the absorbance values of the radical anion surviving at 20 μs after the electron pulse were measured at 620 nm and plotted as a function of pH and fitted to eq i.³⁷ The inset of Figure 1A represents such a plot obtained for PABP.

$$A_{\text{obs}} = \frac{A_{\text{II}}}{1 + 10^{(\text{pH}-\text{p}K_a)}} + \frac{A_{\text{III}}}{1 + 10^{(\text{p}K_a-\text{pH})}} \quad (\text{i})$$

Here, A_{II} and A_{III} represent the absorbance of the species II and III, respectively, at 620 nm at the pH where these are the only absorbing species in the solution. The pK_a values thus obtained for the ABP's have been listed in Table 1. The higher pK_a value of the ketyl radical species of PABP, DMABP, and MK, as compared to that of BP (pK_a 9.2),^{30a} can be explained by the fact that in the case of ABP's, the release of a proton to form the anion radical species may not be a favorable process, due to increased charge density on the carbonyl oxygen, because of the electron-donating effect of the amino and dimethylamino substituents as well as the highly stabilized charge-transfer type valence bond structures of these ketones.¹⁹ However, the pK_a value for the ketyl radical of OABP (8.8) is lower than that of PABP (9.8), probably because of increased stabilization of the resultant anion radical species due to formation of an intramolecular hydrogen bond.¹⁹

(b) Cation Radicals. The triplet states of DMABP and MK have been shown to act as an electron donor to a number of cationic dyes.³⁸ However, no attempt has been made to characterize the cation radical species thus formed in these electron-transfer reactions. Detection of the cationic species in any photochemical or radiation chemical process reveals the involvement of charge- or electron-transfer interaction between the reactants with certainty. Hence it is essential to have information regarding the spectroscopic and kinetic properties of the cation radical by generating it in an isolated condition. The electron pulse radiolysis in chlorinated solvents has been used as a standard method to generate and characterize the radical cations of different kinds of solute molecules.^{39,40} However, in this method, several other oxidants are generated in solution, in addition to the radical cation of the solvent molecule, which is the main oxidant. Different kinds of transient species, such as ion pairs, radicals, and chlorine atom adducts, may be formed. Hence this method becomes nonselective and one should be careful in characterizing the transient species formed in these experiments.

We have studied the oxidized species generated by pulse radiolysis of the ABP's in two chlorinated solvents, namely, tetrachloromethane (TCM) and 1,2-dichloroethane (DCE), the dielectric constant values of which are 4 and 10, respectively. In TCM the main oxidizing species are $CCl_4^{\bullet+}$ ($G = 1.6 \pm 0.4$ per 100 eV), $\bullet CCl_3$ ($G \sim 0.75$ per 100 eV), and $\bullet Cl$.³⁹ The two transient oxidant species, $CCl_4^{\bullet+}$ and $\bullet CCl_3$, react with aromatic solutes to generate the cation radical of the latter but $\bullet Cl$ reacts with the solute to form an ion-pair complex or adduct or abstracts a hydrogen atom to form the neutral radical species.³⁹ However, in DCE, there are several kinetically distinguished cationic species of the solvent, which react selectively with different kinds of solutes.⁴⁰

In the case of the electron pulse radiolysis of DMABP in TCM, the transient absorption spectrum recorded at 0.5 μs shows a band having maximum absorption at 610 nm (curve a in Figure 2). The transient absorption monitored at this wavelength decays mainly by first-order kinetics with lifetime of $0.5 \pm 0.1 \mu s$, leaving very little residual absorption after 1 μs . The spectrum (curve b) of the transient species observed at 2 μs after the electron pulse could be assigned to the free cation radical of DMABP ($DMABP^{\bullet+}$) in TCM, escaping geminate recombination. Hence the ion pair [$DMABP^{\bullet+} \cdot Cl^-$] is the main transient species formed in this solvent and the geminate recombination is the major process undergone by the ion pair. In DCE, the spectrum of the transient species recorded at 0.5 μs (curve c) has a maximum at 630 nm and the spectrum is broader as compared to that obtained in TCM. At later time the absorption

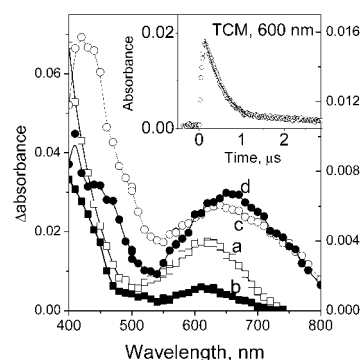


Figure 2. Time-resolved absorption spectra of the transient species produced due to pulse radiolysis of DMABP (5×10^{-3} mol dm^{-3}) in TCM solution recorded at 0.5 (a) and 2 μs (b) and in DCE solution at 0.5 (c) and 20 μs (d) after the electron pulse. The inset shows the kinetic trace recorded at 600 nm for TCM solution.

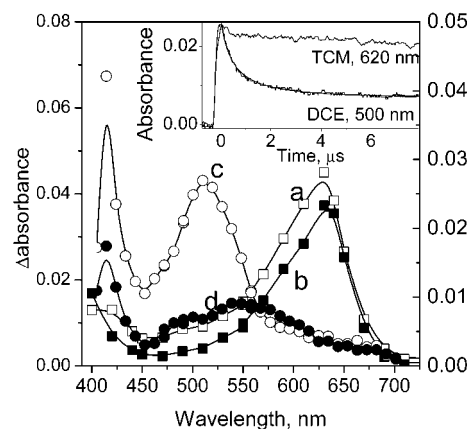


Figure 3. Time-resolved absorption spectra of the transient species produced due to pulse radiolysis of MK (5×10^{-3} mol dm^{-3}) in TCM solution recorded at 0.5 (a) and 10 μs (b) and in DCE solution at 0.5 (c) and 18 μs (d) after the electron pulse. The inset shows the kinetic traces recorded at 500 nm for DCE solution and at 620 nm for TCM solution. The initial fast order decay in each case indicates the geminate recombination process, taking place in the ion pair.

maximum shifts to 650 nm (curve d). The transient absorption shows a small growth while monitored at 650 nm but at a longer time scale the transient absorption decays following second-order kinetics ($2k/\epsilon = (1.8 \pm 0.5) \times 10^6$ $cm^2 s^{-1}$). These facts probably indicate that due to pulse radiolysis of DMABP in DCE, both the ion pair [$DMABP^{\bullet+} \cdot Cl^-$] as well as the free cation radical, $DMABP^{\bullet+}$, are formed. The small growth observed at 650 nm is probably due to formation of free $DMABP^{\bullet+}$, which escape geminate recombination. The 30 nm red shift in the maximum of the absorption spectrum of $DMABP^{\bullet+}$ in DCE with respect to that in TCM could be assigned to higher polarity of DCE. A few reasons may be ascribed to the higher yield of formation of ion pair in TCM as compared to that in DCE. They are lower polarity, higher Cl atom content and the longer lifetime of the $\bullet Cl$ atom radical in TCM (172 ns) as compared to that in DCE (7–10 ns).⁴⁰

While MK is radiolyzed by electron pulses in TCM, the only transient species observed at 0.5 μs has the absorption maximum at 630 nm, but this peak position shifts to the red by about 5 nm when observed at 10 μs (Figure 3). The transient absorption monitored at 620 nm shows very little initial fast decay (within about 1.5 μs , inset of Figure 3). At longer time domain the transient species decay following second-order kinetics with decay rate constant, $2k/\epsilon = (6.0 \pm 0.5) \times 10^5$ $cm^2 s^{-1}$. The very fast initial decay could be assigned to the geminate recombination in ion pair [$MK^{\bullet+} \cdot Cl^-$], which is formed by the recombina-

tion reaction between MK and $\cdot\text{Cl}$. The longer-lived transient could be assigned to the cation radical of MK, $\text{MK}^{\bullet+}$, which has escaped geminate recombination or formed directly due to interaction between MK and the radical cation of the solvent, $\text{CCl}_4^{\bullet+}$. However, in DCE, the transient absorption recorded at 0.5 μs after the electron pulse has the absorption maxima at ca. 400 and 500 nm and after about 10 μs , we observe a new transient absorption spectrum developing with maximum at ca. 540 nm. The transient species, having the absorption maximum with a large blue shift as compared to that of the cation radical in a more polar solvent could not be assigned to the ion pair $[\text{MK}^{\bullet+} \cdot \text{Cl}^-]$ but probably some kind of chlorine atom adduct. We are not certain about its identity.

(c) Triplet State. Pulse radiolysis is an excellent technique for selective creation of the excited triplet states of organic molecules using the triplet-triplet energy-transfer method in aromatic solvents such as benzene.⁴¹ We showed in earlier sections that due to pulse radiolysis in haloalkanes and water, ions and radicals, respectively, could easily be generated and used for the time-resolved study of electron- and proton-transfer processes. However, in the pulse radiolysis of benzene, formation of singlet and triplet excited states are the major processes. The radiolysis of benzene produces the benzene triplet (^3BZ) of very high energy (353 kJ mol^{-1}) in high yield. ^3BZ can transfer its energy to another solute having $E_T < 353 \text{ kJ mol}^{-1}$, thus generating the triplet state of the latter. Hence, in the pulse radiolysis of benzene containing a relatively higher concentration ($\sim 10^{-3} \text{ mol dm}^{-3}$) of scavenger species, the ^3BZ can serve as a sensitizer for initiating the triplet-triplet energy-transfer process.⁴¹ The low intersystem crossing efficiency for the conversion of the singlet to the triplet state of the solute molecule does not pose any limitation to the production of the triplet state. Also, the triplet production process being selective, conclusive evidence for the assignment of the photolytically generated transient species to the triplet state can be obtained from the pulse radiolysis studies of the solutes in deaerated solutions of benzene.

The time-resolved spectra of the transients produced due to electron pulse radiolysis of the four ABP's (concentration $\sim 10^{-3} \text{ mol dm}^{-3}$) in deaerated benzene solutions are presented in the Figures 4 and 5. The spectra represented by the curves denoted by a, recorded at about 0.5 μs after the electron pulse, could be assigned to the triplet states of these molecules. The spectra for PABP and MK have been seen to be very similar to those reported earlier from flash photolysis experiments.^{19b,c} We observe the only absorption band of the OABP triplet ($^3\text{OABP}$) in the 450–600 nm region with a maximum at ca. 500 nm (Figure 4A). However, the triplet state of each of the other three derivatives of benzophenone studied here has another broad absorption band in the region 600–850 nm, in addition to the one at the ca. 450–600 nm region. $^3\text{OABP}$ decays to the ground state without producing any other transient species. However, in the case of PABP, DMABP, or MK, the transient absorption spectra recorded at a longer time domain, e.g., later than 10 μs after the electron pulse, reveal the production of another transient species that has absorption maxima at ca. 410 and 560 (PABP, Figure 4B) or 600 nm (DMABP and MK, Figure 5).

The lifetimes of the triplet states could be determined by monitoring the clean first-order decay of the transient absorption either at 500 nm (for $^3\text{OABP}$), 700 nm (for ^3MK), or 750 nm (for $^3\text{PABP}$ and $^3\text{DMABP}$). $^3\text{OABP}$ is short-lived and the lifetime is only $0.6 \pm 0.03 \mu\text{s}$. The reason is probably the very fast energy relaxation process via hydrogen stretching vibrations in the intramolecular hydrogen bond.⁴² The lifetimes of the triplet states of the other three derivatives have been found to be

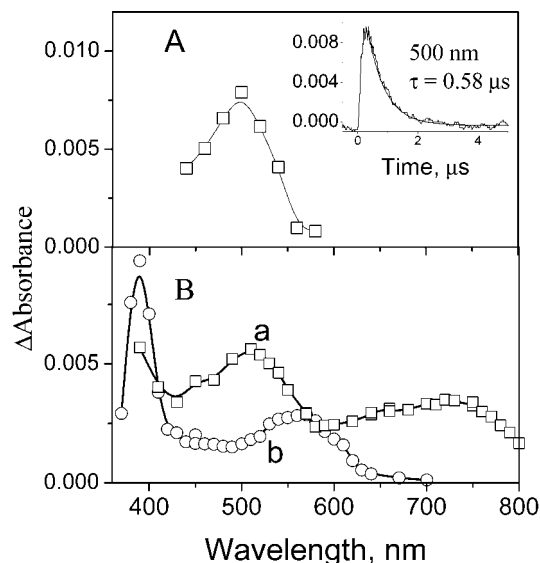


Figure 4. (A) Absorption spectrum of the triplet state of OABP produced due to pulse radiolysis of $1 \times 10^{-3} \text{ mol dm}^{-3}$ OABP in benzene solution. The inset shows the decay of the triplet state. (B) Time-resolved spectra of the transient species produced due to pulse radiolysis of $1 \times 10^{-3} \text{ mol dm}^{-3}$ PABP in benzene solution recorded at 0.5 (a) and 10 μs (b), assigned to the triplet state and the ketyl radical species (type III), respectively.

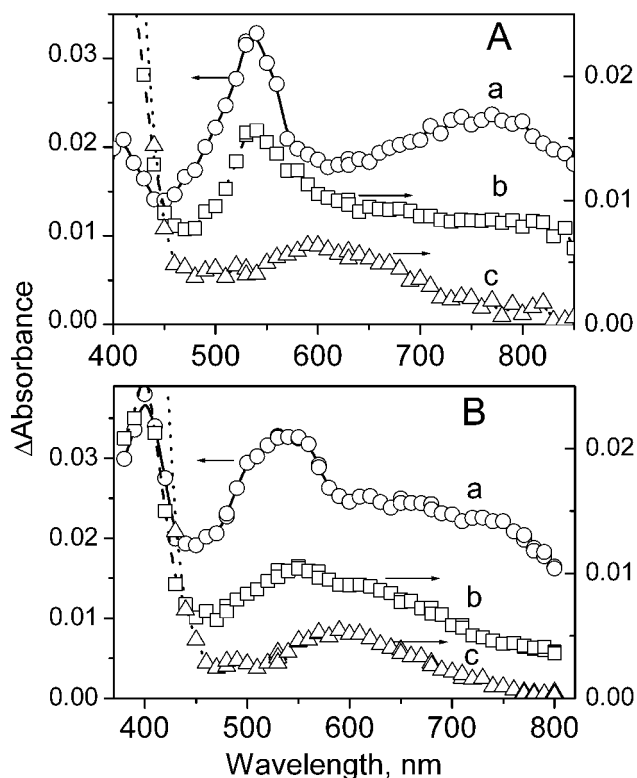


Figure 5. Time-resolved transient absorption spectra obtained due to pulse radiolysis of $1 \times 10^{-2} \text{ mol dm}^{-3}$ (A) DMABP (with time windows 0.5 (a), 4 (b), and 10 (c) μs) and (B) MK (with time windows 0.5 (a), 2 (b), and 4 (c) μs) in benzene solution.

sensitive to the concentration of the ground state used; i.e., the triplet state is self-quenched by its ground state. Hence the pseudo-first-order lifetimes have been determined by monitoring the decay of the transient absorption at 700 or 750 nm with different ground-state concentrations of the solutes varying in the range from 1×10^{-5} to $2 \times 10^{-2} \text{ mol dm}^{-3}$. The rates of the decay of the triplet states (i.e., the inverse of the lifetime)

TABLE 2: Triplet-State Characteristics of ABP's and Their Photochemical Reactions with Benzophenone in Benzene

ABP	E_T , eV	$E_{ox}^{1/2}$, V	$\Delta G_{et}({}^3BP-ABP)$, eV	λ_{max} , nm	ϵ , $dm^3 mol^{-1} cm^{-1}$ (λ)	τ_T , μs	k_{SQ} , $10^7 dm^3 mol^{-1} s^{-1}$	k_Q , $10^9 dm^3 mol^{-1} s^{-1}$	mechanism of quenching
OABP	3.0	1.23	+0.06	500		0.6 ± 0.2		3.7 ± 0.5	energy transfer
PABP	2.9	1.25	+0.08	550, 750		3.2 ± 0.5	8.0 ± 0.6	2.7 ± 0.5	atom transfer
DMABP	2.7	1.08	-0.09	530, 750	6700 ± 1000 (750)	12.0 ± 0.5	6.25 ± 0.5	4.2 ± 0.5	electron & proton transfer via exciplex formation
MK	2.7	0.95	-0.22	530, 700 (sh)	7500 ± 1000 (700)	11.4 ± 0.5	1.51 ± 0.3	2.6 ± 0.5	electron & proton transfer

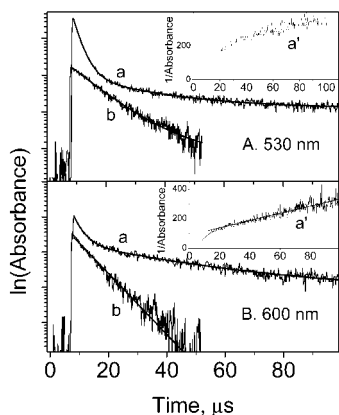
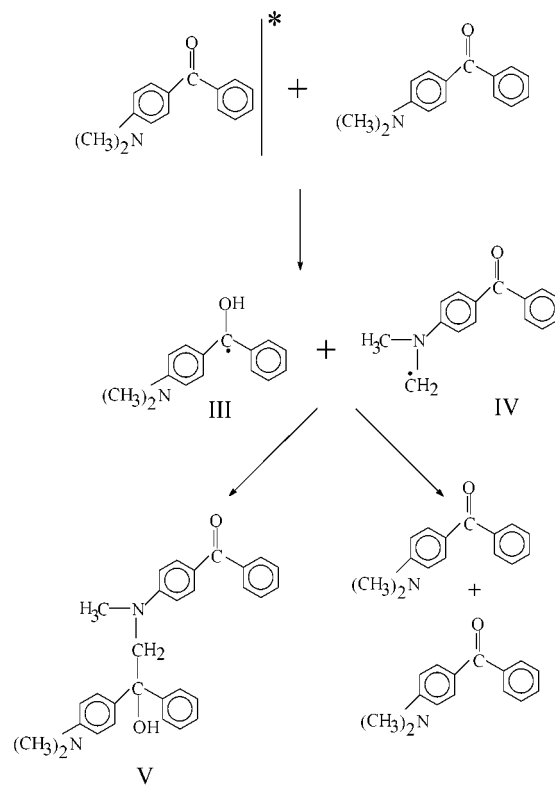


Figure 6. Decay profiles of the transient species produced due to pulse radiolysis of (a) $2 \times 10^{-2} mol dm^{-3}$ and (b) $1 \times 10^{-3} mol dm^{-3}$ DMABP in benzene, recorded at (A) 530 nm and (B) 600 nm. The fit functions are also shown. Decay profiles represented by curves 'a' have been fitted with a dual exponential fit function, while those represented by the curves 'b' have been shown to be well fitted by a single-exponential fit function. The curves represented by 'a' in the insets show the fittings of the decay profiles 'a' to the second-order decay function.

have been seen to increase linearly with an increase in concentration of the solute. The intrinsic lifetimes of the triplet states (τ_T , the lifetime in absence of self-quenching) and the rates of self-quenching interaction (k_{SQ}) have been obtained from the intercept and the slope of the linear plots, respectively. These values have been given in Table 2 and they agree well with those determined by our flash photolysis measurements.^{19b,44} Earlier, several authors reported the self-quenching interaction of the triplet states of PABP and MK.^{26,43} However, our values are about one order of magnitude lower than the reported values. The lifetime value for 3MK determined by us is also found to be much shorter than the values, which are found to vary from 19 to 43 μs , reported earlier by different groups (ref 26 and the references therein). The reason for obtaining a longer lifetime in the earlier studies by flash photolysis measurements may possibly be due to the presence of the longer-lived component having an absorption band in the 500–700 nm region.

The kinetic behaviors of the absorption decay profiles for 3DMABP and 3MK monitored at different wavelengths are different and complicated, as shown in Figure 6. While the concentration of DMABP or MK used was below $5 \times 10^{-3} mol dm^{-3}$, the decay of the transient species measured at any of the wavelengths on its spectrum could be well-fitted by a single-exponential decay function (curve b). At higher concentrations ($> 5 \times 10^{-3} mol dm^{-3}$), the transient absorption at ca. 530 or 600 nm shows a multicomponent decay (curve a). Although, at either of the wavelengths, the lifetime of the shorter first-order component is equal to the lifetime of the triplet state (measured at 700 or 750 nm), the kinetics of the longer component could be fitted either by first-order or second-order or both depending on the concentration of the ketones used. Complicated kinetic behavior of the transient species surviving

SCHEME 2



beyond 10 μs time domain, monitored at different wavelengths, indicates that the spectra recorded beyond 10 μs time domain (curves c in Figure 5) are due to the presence of more than one species and also they follow more than one kind of reaction path to decay.

The self-quenching reaction of the triplet state of ABP's could be represented by the Scheme 2, following the reaction scheme suggested by Wamser et al. who studied the interaction between 3BP and MK in benzene.³¹ The absorption band with maximum at 600 nm (spectra c in Figure 5) is assigned to the radical of the type IV. Formation of the radical type IV in the photochemical self-quenching interaction in the case of DMABP and MK has been confirmed by trapping it by nitrosobutyl chloride and detected by ESR.⁴⁵ However, in the above reaction, formation of the radical of type IV should be accompanied by the formation of the radical of type III, having absorption maxima at 580 nm for MK and 550 nm for DMABP (Table 1). Hence, the broad absorption band with a maximum at ca. 600 nm could be assigned to the presence of both the radicals of types III and IV. However, in the case of PABP, we observe the formation of the ketyl radical only (radical of type III), having an absorption maximum at 550 nm (curve b in Figure 4B), and it is very similar to the one recorded in the electron reaction with PABP at pH 5 (Figure 1A). We could not observe any other transient species, which could be assigned to the counter radical (type IV) formed due to release

of a hydrogen atom from the amino group of PABP molecule in the ground state.

To explain the mechanism of self-quenching reactions in ABP's, Schuster et al. predicted the formation of triplet excimer involving charge resonance as the stabilizing factor, but their efforts to characterize the triplet excimer species were not successful.²⁶ We reported earlier that the shapes or characteristics of the absorption spectra of the triplet state generated by laser pulse excitation were sensitive to the concentration of MK used in flash photolysis experiments.^{19c} However, we attributed this change of spectral shapes to some kind of association in the ground state via formation of aggregates and excluded the possibility of any kind of association between the T_1 state and the ground-state molecule. The driving force for the charge-transfer interaction in the self-quenching reaction is given by eq ii. The values of $E_{ox}^{1/2}$ (ABP) and E_T (ABP) determined in this work are given in Table 2. We could not determine the $E_{red}^{1/2}$ (ABP) values using our cyclic voltammeter due to its technical limitation. However, it is expected that the values should be less than that of BP (-1.83 eV). Using eq ii, the lowest possible value of ΔG_{et} could be calculated and this showed that the self-quenching reaction of the triplet state via charge-transfer mechanism is not thermodynamically feasible for any of the ABP's. Hence, the probable mechanism operating in the self-quenching process is the simple hydrogen atom abstraction reaction by the $n\pi^*$ T_1 state, which is either the lowest triplet state or energetically very close to the lower lying $\pi\pi^*$ T_1 state and is populated significantly even at ordinary temperature.^{19b,c}

$$\Delta G_{et}(\text{self-quenching}) =$$

$$E_{ox}^{1/2}(\text{ABP}) - E_{red}^{1/2}(\text{ABP}) - E_T(\text{ABP}) \quad (\text{ii})$$

(d) Interaction between ^3BP and ABP's. To gain further insight into the mechanism and the kind of interaction involved in the self-quenching reaction and the role of the triplet excimer or exciplex, we investigated the interaction between two nonidentical ketones or ketone derivatives so as to be able to understand the role of different kinds of excited states or radicals, which are produced in this process. We have studied the nature of interaction between ^3BP and the ground state of each of the four ABP's. ^3BP has $n\pi^*$ character. Its energy and electron affinity are higher than those of the amino-substituted BP derivatives used here. Wamser et al.³¹ predicted, without any experimental evidence, that the photoreaction between ^3MK and BP proceeds via formation of a triplet exciplex. We have shown earlier that the self-quenching of ^3MK is a predominant process contributing towards its decay. In this study, we are able to avoid the self-quenching interaction between the triplet and the ground state, since the self-quenching rate is slow for ^3BP ($\sim 10^5 \text{ dm}^3 \text{ mol}^{-1} \text{ s}^{-1}$).^{26,29} The pulse radiolysis technique has the advantage over the flash photolysis technique in selective production of ^3BP just by using a higher concentration (about 20 times higher) of BP than that of ABP. Since the absorption spectra of ABP's are red-shifted as compared to that of BP, selective excitation of BP is not possible in the presence of ABP's in flash photolysis experiments. We have observed that the nature of interaction between ^3BP and the derivative molecules have been different in each case. We have been able to vary the free energy change for the charge- or electron-transfer reaction (determined using eq iii and the values $E_{red}^{1/2}(\text{BP}) = -1.83 \text{ V}^{4a}$ and $E_T(\text{BP}) = 3.0 \text{ eV}^{38}$) in a systematic manner while maintaining the nature of the excited state the same, i.e., $n\pi^*$ for ^3BP . Hence we have been able to

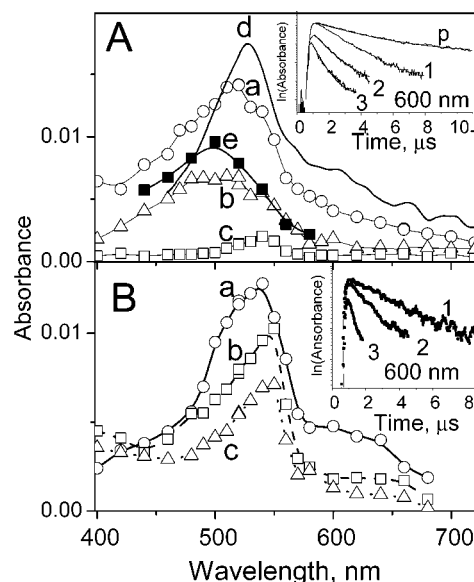


Figure 7. Time-resolved absorption spectra of the transients produced due to pulse radiolysis of $1 \times 10^{-2} \text{ mol dm}^{-3}$ BP in benzene in the presence of $5 \times 10^{-4} \text{ mol dm}^{-3}$ OABP (A) and PABP (B). In both cases the spectra are recorded at 0.4 (a), 1 (b), and 10 (c) μs after the electron pulse. In (A), the absorption spectra due to ^3BP (d) as well as $^3\text{OABP}$ (e) are also shown. The insets show the decay of ^3BP monitored at 600 nm in the presence of 0.05 (1), 0.1 (2), and 0.5 (3) $\times 10^{-3} \text{ mol dm}^{-3}$ OABP or PABP. Decay profile p represents the decay of ^3BP only. The concentration of BP was kept constant ($1 \times 10^{-2} \text{ mol dm}^{-3}$) in each measurement.

see a change in reaction mechanism that could be correlated with the electron-donating abilities of the ABP's.

$$\Delta G_{et}(^3\text{BP-ABP}) =$$

$$E_{ox}^{1/2}(\text{ABP}) - E_{red}^{1/2}(\text{BP}) - E_T(\text{BP}) \quad (\text{iii})$$

Figure 7A represents the time-resolved spectra of the transients produced due to pulse radiolysis of a solution containing $1 \times 10^{-2} \text{ mol dm}^{-3}$ BP and $5 \times 10^{-4} \text{ mol dm}^{-3}$ OABP in benzene. Since the concentration of BP is about 20 times higher than that of OABP, energy of ^3BZ is preferentially transferred to ^3BP rather than to $^3\text{OABP}$. We also observed that $^3\text{OABP}$ produced in pulse radiolysis of a solution containing only $5 \times 10^{-4} \text{ mol dm}^{-3}$ OABP was negligible. Hence ^3BP should be the only transient species formed in the process of energy transfer from ^3BZ to the solutes present in the solution. However, the absorption spectrum recorded at 0.4 μs after the electron pulse showed a peak at 510 nm and it was a little different from that of ^3BP . The spectrum of ^3BP , which has been obtained by electron pulse radiolysis of BZ in the presence of only $1 \times 10^{-2} \text{ mol dm}^{-3}$ BP, is also shown in the same figure for comparison (curve d). It has a maximum at 530 nm and a shoulder at 600 nm. Absorbance at 600 nm decays following first-order decay law with a lifetime of 0.65 μs . This is much shorter than the lifetime of ^3BP (3.5 μs), which has been measured in the absence of OABP (decay trace p in the inset of Figure 7A). The transient absorption spectrum (curve b) recorded at 1 μs after the electron pulse has the distinct peak at 500 nm, and this spectrum is very similar to that of $^3\text{OABP}$. The spectrum recorded after 10 μs indicates a very little residual absorption with a peak at 545 nm, which is characteristic of the ketyl radical of BP. Hence it becomes evident that the energy transfer from ^3BP to $^3\text{OABP}$ is the major deactivation process for ^3BP , which is quenched by OABP very efficiently. The energy-transfer rate, which could be calculated from the slope

of the linear plot of the pseudo-first-order rates monitored at 600 nm against the concentrations of OABP, is given in Table 2.

Figure 7B shows the time-resolved absorption spectra of the transients produced due to pulse radiolysis of the solution containing $1 \times 10^{-2} \text{ mol dm}^{-3}$ BP and $5 \times 10^{-4} \text{ mol dm}^{-3}$ PABP in benzene. The transient spectrum recorded at $0.4 \mu\text{s}$ after the electron pulse has a maximum at ca. 540 nm and shoulders at 530 and 600 nm. The absorbance monitored at 600 nm decays very fast following first-order kinetics with a lifetime of $0.5 \mu\text{s}$. However, the decay monitored at 530 nm follows mixed-order kinetics. The initial short first-order component decays with the same lifetime ($0.5 \mu\text{s}$) as that obtained by monitoring the transient absorbance decay at 600 nm, and the longer second-order component decays with the rate constant, $2k/\epsilon$ value of $5 \times 10^5 \text{ cm}^{-1}$. The first-order decay monitored at 600 nm could be assigned to the decay of ^3BP , and the transient, surviving at longer time having a peak at 545 nm, to the BP ketyl radical, the decay rate of which has been calculated to be $1.8 \times 10^9 \text{ dm}^3 \text{ mol}^{-1} \text{ s}^{-1}$ using $\epsilon_{545} = 3500 \text{ dm}^3 \text{ mol}^{-1} \text{ cm}^{-1}$.^{36a} The formation of the ketyl radical of BP with relatively higher yield (than that in the case of the BP-OABP system) is indicative of a hydrogen-atom-transfer reaction from the PABP molecule in the ground state to ^3BP . The formation of the ketyl radical of BP is also possible via electron transfer from the PABP molecule to ^3BP followed by proton transfer. But as Table 2 shows, this reaction is not feasible due to the positive free energy change for the electron-transfer reaction. In this case, the fact that the energy transfer from ^3BP to PABP is not an important process for the decay of ^3BP is evident from the absence of any transient absorption in the 600–850 nm wavelength region, which would be the characteristic of $^3\text{PABP}$ (Figure 4B). The hydrogen-atom-transfer rate could be determined from the slope of the linear plot of the pseudo-first-order rates monitored at 600 nm as a function of concentration of PABP, to be $4 \times 10^9 \text{ mol}^{-1} \text{ dm}^3 \text{ s}^{-1}$. In this case, we could not observe the formation of the exciplex between ^3BP and PABP. Hence we predict that the mechanism of the reaction between ^3BP and PABP can be described by simple hydrogen atom abstraction via free radical mechanism.^{2c,24}

Figure 8A shows the absorption spectra of the transients produced due to pulse radiolysis of the solution containing $1 \times 10^{-2} \text{ mol dm}^{-3}$ BP and $5 \times 10^{-4} \text{ mol dm}^{-3}$ DMABP. Each of the absorption spectra recorded at 0.4 and $2 \mu\text{s}$ after the electron pulse shows a peak at 540 nm, and a very broad absorption band in the 600–850 nm region. These are very similar to that due to $^3\text{DMABP}$ (Figure 5A), but no distinct maximum has been seen in the 600–800 nm region. The spectra recorded at 6 and $18 \mu\text{s}$ have two distinct bands. One of them has a maximum at ca. 545 nm, which is characteristic of the ketyl radical of benzophenone. The other has a maximum at ca. 620 nm. Since we have argued earlier that the probability of formation of $^3\text{DMABP}$ by direct energy transfer from ^3BZ in the present experimental condition is negligibly small, $^3\text{DMABP}$ could not be produced by direct energy transfer from ^3BZ , but via some kind of interaction between ^3BP and the ground state of DMABP. This has been confirmed by observing the slower growth of the transient absorption at 750 nm at lower concentrations of DMABP used in the solution. The inset of Figure 8A shows the temporal evolution of the transient absorption monitored at 750 nm obtained by radiolysis of solutions containing $1 \times 10^{-2} \text{ mol dm}^{-3}$ BP and different concentrations of DMABP in the range 5×10^{-5} to $5 \times 10^{-4} \text{ mol dm}^{-3}$ in benzene. At lower concentrations of DMABP, e.g., 5×10^{-5}

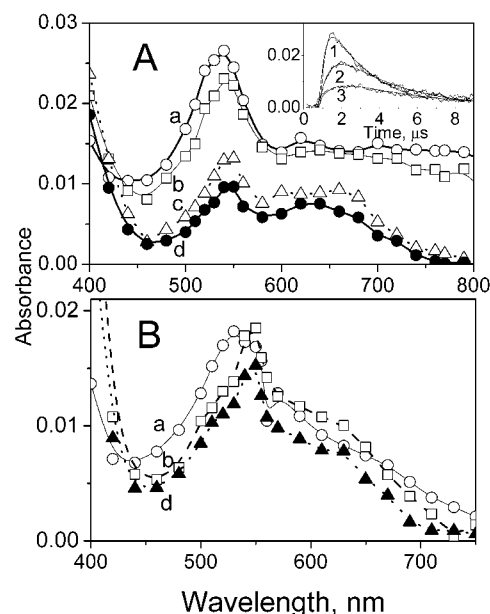


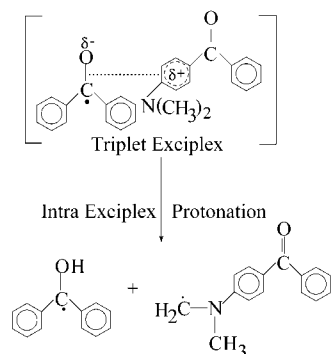
Figure 8. Time-resolved absorption spectra of the transients produced due to pulse radiolysis of $1 \times 10^{-2} \text{ mol dm}^{-3}$ BP in benzene in the presence of $5 \times 10^{-4} \text{ mol dm}^{-3}$ (A) DMABP and (B) MK. In both cases the spectra are recorded at (a) 0.4, (b) 2, (c) 6, and (d) $18 \mu\text{s}$ after the electron pulse. The inset shows the growth and decay of the transient species monitored at 750 nm in the presence of (1) 0.5, (2) 0.1, and (3) $0.05 \times 10^{-3} \text{ mol dm}^{-3}$ DMABP. The concentration of BP was kept constant ($1 \times 10^{-2} \text{ mol dm}^{-3}$) in each measurement.

mol dm^{-3} , the transient absorption shows a growth followed by decay. The curves were fitted with a function having each one of the growth and decay components, the lifetimes of both of which were found to depend on the concentration of DMABP in solution. However, the possibility that the transient observed at $0.4 \mu\text{s}$ after the electron pulse is due to $^3\text{DMABP}$, formed by energy transfer from ^3BP , is also excluded from the fact that the shape of this spectrum in the 600–850 nm region is very different from that of $^3\text{DMABP}$. Hence, this transient could possibly be assigned to the formation of triplet exciplex, which is having both excitation resonance and charge-transfer contributions, $[\text{DMABP}\cdot\cdot\text{BP}^*] \leftrightarrow [\text{DMABP}^*\cdot\text{BP}] \leftrightarrow [\text{DMABP}^+\cdot\text{BP}^-]$.

The absorbance at 750 nm decays fast due to intra-exciplex proton transfer to form the ketyl radical of BP having a maximum at 545 nm and the radical of type IV, as mentioned earlier, having an absorption maximum at 640 nm. The CT type interaction has been seen to be thermodynamically feasible from calculation of free energy change for the ET reaction between ^3BP and DMABP (Table 2). The decay kinetics of the transient absorption was also followed at 530 and 640 nm. At these wavelengths, the decay kinetics showed two components. The faster component is single exponential, having a lifetime nearly equal to that of the exciplex decay monitored at 750 nm. However, the slower component could be fitted both by single exponential as well as second-order decay law. Hence, as mentioned earlier, it is probably the combination of two different decay processes undergone by the radicals produced via the intra-exciplex proton-transfer process. The interaction between ^3BP and DMABP may be represented by Scheme 3.

In Figure 8B we present the results of the pulse radiolysis experiment concerned with the interaction behavior between ^3BP and MK in benzene solution. In this experiment, however, we could not observe the formation of the exciplex, but only the formation of the ketyl radical of BP and the radical of type IV derived from MK having a maximum at ca. 600 nm. The decay kinetics of the transient species were monitored at 530

SCHEME 3



and 640 nm using 1×10^{-2} mol dm⁻³ BP and different concentrations of MK varying in the range $(0.5-5) \times 10^{-4}$ mol dm⁻³. The kinetic behavior of the transient species was very similar to that observed in the case of the BP-DMABP system. The negative free energy change of electron transfer (ET) from ³BP to MK (Table 2) indicates that the interaction between these two species, taking place via electron transfer followed by proton transfer, is thermodynamically feasible. Since we could not detect an absorption band either due to the cation radical of MK ($\lambda_{\max} \sim 650$ nm) or the anion radical of BP ($\lambda_{\max} \sim 690$ nm),³⁵ the electron-transfer and the subsequent proton-transfer processes could not be separated from each other. The proton-transfer process is strongly coupled to the electron-transfer process, and hence the former is too fast to allow the detection of the cation and anion radicals. The rate of the coupled electron- and proton-transfer process has been determined from the slope of the linear plot of the pseudo-first-order rates measured at 530 nm as a function of concentration of MK and has been given in Table 2.

In conclusion, we confirm that in self-quenching interaction between the triplet state of ABP and its ground state, the $n\pi^*$ triplet plays the major role and no triplet exciplex formation is involved. This is in contradiction to the predictions made from the earlier studies. The $n\pi^*$ triplet state of benzophenone reacts with ABP's either by energy transfer (in the case of OABP) or by hydrogen atom abstraction reaction (in the case of PABP) or by charge-transfer coupled with proton-transfer (in the case of DMABP and MK) mechanism. Exciplex formation, as an intermediate of the reaction, has been evident only in the case of interaction between ³BP and DMABP.

Acknowledgment. We gratefully acknowledge help from Mr. V. N. Rao and his colleagues in conducting pulse radiolysis experiments and Dr. G. Venkateswaran for cyclic voltammetric measurements. We also thank the referees for making very useful suggestions for improving the presentation.

References and Notes

- (1) (a) Hoshino, H.; Shizuka, H. In *New Aspects of Radiation Curing in Polymer Science and Technology*; Fonassier, J. P., Rabeck, J. F., Eds.; Elsevier: Amsterdam, 1993; Vol. 2, p 637. (b) Hoshino, H.; Shizuka, H. In *Photoinduced Electron Transfer*; Fox, M. A., Chanon, N., Eds.; Elsevier: Amsterdam, 1988; Part C. p 513. (c) Gilbert, A.; Baggot, J. *Essentials of Molecular Photochemistry*; CRC Press: Boston, 1991; p 302-328. (d) Scuster, D. I.; Karp, P. B. *J. Photochem.* **1980**, *12*, 333.
- (2) (a) Wagner, P. J. *Top. Curr. Chem.* **1976**, *66*, 1. (b) Wagner, P. J.; Park, B. S. *Org. Photochem.* **1991**, *11*, 227. (c) Griller, D.; Howard, J. A.; Marriott, P. R.; Scaiano, J. C. *J. Am. Chem. Soc.* **1981**, *103*, 619.
- (3) (a) Wagner, P. J.; Truman, R. J.; Scaiano, J. C. *J. Am. Chem. Soc.* **1985**, *107*, 7093. (b) Scaiano, J. C. *J. Photochem.* **1973**, *2*, 81.
- (4) (a) Wagner, P. J.; Truman, R. J.; Puchalski, A. E.; Wake, R. J. *Am. Chem. Soc.* **1986**, *108*, 7727. (b) Wagner, P. J.; Thomas, M. J.; Puchalski, A. E. *J. Am. Chem. Soc.* **1986**, *108*, 7739. (c) Wagner, P.; Leavitt, R. A. *J. Am. Chem. Soc.* **1973**, *95*, 3669.
- (5) Das, P. K.; Encinas, M. V.; Scaiano, J. C. *J. Am. Chem. Soc.* **1981**, *103*, 4154.
- (6) Leigh, W. J.; Lathioor, E. C.; St. Pierre, M. J. *J. Am. Chem. Soc.* **1996**, *118*, 12339.
- (7) Naguib, Y. M. A.; Steel, C.; Cohen, S. G.; Young, M. A. *J. Phys. Chem.* **1987**, *91*, 3033.
- (8) Bobrowski, K.; Marciniak, B.; Hug, G. L. *J. Am. Chem. Soc.* **1992**, *114*, 10279.
- (9) (a) Peters, K. S.; Lee, J. *J. Phys. Chem.* **1993**, *97*, 3761. (b) Simon, J. D.; Peters, K. S. *J. Am. Chem. Soc.* **1981**, *103*, 6403. (c) Simon, J. D.; Peters, K. S. *J. Am. Chem. Soc.* **1982**, *104*, 6542. (d) Simon, J. D.; Peters, K. S. *J. Phys. Chem.* **1983**, *87*, 4855.
- (10) Gramain, J. C.; Remuson, R. *J. Org. Chem.* **1985**, *50*, 1120.
- (11) Wang, S. K. *J. Am. Chem. Soc.* **1978**, *100*, 5488.
- (12) Roth, H. D.; Manion, M. L. *J. Am. Chem. Soc.* **1975**, *97*, 6886.
- (13) (a) Arimitsu, S.; Masuhara, H.; Mataga, N.; Tsubomura, H. *J. Phys. Chem.* **1975**, *79*, 1255. (b) Miyasaka, H.; Morita, K.; Kamoda, K.; Mataga, N. *Bull. Chem. Soc. Jpn.* **1990**, *63*, 3385; *Chem. Phys. Lett.* **1991**, *178*, 504.
- (14) Cohen, S. G.; Parola, A.; Parsons, G. H. *Chem. Rev.* **1973**, *73*, 141.
- (15) Kavarnos, G. J.; Turro, N. J. *Chem. Rev.* **1986**, *86*, 401.
- (16) (a) Wagner, P. J.; Leavitt, R. A. *J. Am. Chem. Soc.* **1970**, *92*, 5806. (b) Wagner, P. J.; Lam, H. M.-H. *J. Am. Chem. Soc.* **1980**, *102*, 4167. (c) Wagner, P. J.; Puchalski, A. E. *J. Am. Chem. Soc.* **1978**, *100*, 5948. (d) Wagner, P. J.; Puchalski, A. E. *J. Am. Chem. Soc.* **1980**, *102*, 6177. (e) Wagner, P. J.; Kempainen, A. E.; Schott, H. N. *J. Am. Chem. Soc.* **1973**, *95*, 5604. (f) Wagner, P. J.; Siebert, E. J. *J. Am. Chem. Soc.* **1981**, *103*, 7329.
- (17) (a) Porter, G.; Suppan, P. *Trans. Faraday Soc.* **1966**, *62*, 3375. (b) Porter, G.; Suppan, P. *Trans. Faraday Soc.* **1965**, *61*, 1664. (c) Beckett, A.; Porter, G. *Trans. Faraday Soc.* **1963**, *59*, 2038.
- (18) (a) Wagner, P. J.; Kempainen, A. E.; Schott, H. N. *J. Am. Chem. Soc.* **1973**, *95*, 5604. (b) Wagner, P. J.; Siebert, E. J. *J. Am. Chem. Soc.* **1981**, *103*, 7329. (c) Wagner, P. J. *Acc. Chem. Res.* **1971**, *4*, 168. (d) Wagner, P. J. *J. Am. Chem. Soc.* **1967**, *89*, 5898. (e) Wagner, P. J.; May, M. J.; Haug, A.; Graber, D. R. *J. Am. Chem. Soc.* **1970**, *92*, 5269. (f) Wagner, P. J.; Kempainen, A. E. *J. Am. Chem. Soc.* **1968**, *90*, 5898. (g) Wagner, P. J.; Kempainen, A. E.; Schott, H. N. *J. Am. Chem. Soc.* **1970**, *92*, 5280. (h) Wagner, P. J.; Schott, H. N. *J. Am. Chem. Soc.* **1969**, *91*, 5383.
- (19) (a) Bhasikuttan, A. C.; Singh, A. K.; Palit, D. K.; Mittal, J. P. *J. Phys. Chem. A* **1998**, *102*, 3470; **1999**, *103*, 4703. (b) Singh, A. K.; Palit, D. K.; Mittal, J. P. *J. Phys. Chem. A* **2000**, *104*, 7002. (c) Singh, A. K.; Palit, D. K.; Mittal, J. P. *Res. Chem. Intermed.* **2001**, *27*, 125.
- (20) (a) Porter, G.; Suppan, P. *Trans. Faraday Soc.* **1966**, *62*, 3375. (b) Porter, G.; Suppan, P. *Trans. Faraday Soc.* **1965**, *61*, 1664.
- (21) Berger, M.; McAlpine, E.; Steel, C. *J. Am. Chem. Soc.* **1978**, *100*, 5147.
- (22) Wolf, W. M.; Brown, R. E.; Singer, L. A. *J. Am. Chem. Soc.* **1977**, *99*, 526.
- (23) (a) Aspari, P.; Ghoneim, N.; Haselbach, E.; Von Raumer, M.; Suppan, P.; Vauthey, E. *J. Chem. Soc., Faraday Trans.* **1996**, *92*, 1689. (b) Ghoneim, N.; Monbelli, A.; Pilloud, D.; Suppan, P. *J. Photochem. Photobiol. A. Chem.* **1996**, *94*, 145.
- (24) Wagner, P. J.; Truman, R. J.; Scaiano, J. C. *J. Am. Chem. Soc.* **1985**, *107*, 7093.
- (25) (a) Scaiano, J. C. *J. Photochem.* **1973/74**, *2*, 81. (b) Turro, N. J.; Dalton, J. C.; Dawes, K.; Farrington, G.; Hautala, R.; Morton, D.; Niemczyk, M.; Schore, N. *Acc. Chem. Res.* **1972**, *5*, 92. (c) Wagner, P. J. *Acc. Chem. Res.* **1971**, *4*, 168. (d) Giering, L.; Berger, M.; Steel, C. *J. Am. Chem. Soc.* **1974**, *96*, 953.
- (26) Scuster, D. I.; Goldstein, M. D.; Bane, P. *J. Am. Chem. Soc.* **1977**, *99*, 187.
- (27) Porter, G.; Suppan, P. *Trans. Faraday Soc.* **1965**, *61*, 1971.
- (28) Schuster, D. I.; Wail, T. M. *J. Am. Chem. Soc.* **1973**, *95*, 4091.
- (29) W. M. Wolf, Legg, K. D.; Singer, L. A.; Parks, J. H. *J. Am. Chem. Soc.* **1975**, *97*, 4490.
- (30) Schuster, D. I.; Goldstein, M. D. *Mol. Photochem.* **1976**, *7*, 209.
- (31) Wamser, C. C.; Hammond, G. S.; Chang, C. T.; Bayer, C., Jr. *J. Am. Chem. Soc.* **1970**, *92*, 6363.
- (32) (a) Guha, S. N.; Moorthy, P. N.; Kishore, K.; Naik, D. B.; Rao, K. N. *Proc. Indian Acad. Sci. (Chem. Sci.)* **1989**, *99*, 261. (b) Mukherjee, T. In *Atomic, Molecular and Cluster Physics*; Ahmed, S. A., Ed.; Narosa: New Delhi, 1997; p 299.
- (33) Baxendale, J. H.; Bussi, F., Eds. *Study of Fast Processes and Transient Species in Pulse Radiolysis*; Reidel: Boston, MA, 1982; (a) p 49, (b) p 297.
- (34) Spinks, J. W. T.; Wood, R. J. *An Introduction to Radiation Chemistry*; Wiley-Interscience: New York, 1990; (a) p 262, (b) p 327.

- (35) Hayon, E.; Ibata, T.; Lichtin, N. N.; Simic, M. *J. Phys. Chem.* **1972**, *76*, 2072.
- (36) Keene, J. P.; Land, E. J.; Swallow, A. J. *J. Am. Chem. Soc.* **1965**, *87*, 5284.
- (37) Land, E. J.; Mukherjee, T.; Swallow, A. J.; Bruce, J. M. *J. Chem. Soc., Faraday Trans. 1* **1983**, *79*, 391.
- (38) Jockusch, S.; Timpe, H.-J.; Schnabel, W.; Turro, N. J. *J. Phys. Chem. A* **1997**, *101*, 440.
- (39) (a) Burrows, H. D.; Grotzinger, D.; Kemp, T. J. *J. Phys. Chem.* **1972**, *76*, 20. (b) Grodkowski, J.; Neta, P. *J. Phys. Chem.* **1984**, *88*, 1405. (c) Emmi, S. S.; Beggiano, G.; Casalbore-Miceli, G. *Rad. Phys. Chem.* **1989**, *33*, 29. (d) Chateaufeuf, J. E. *J. Am. Chem. Soc.* **1990**, *112*, 442.
- (40) Ichinose, N.; Majima, T. *Chem. Phys. Lett.* **2000**, *322*, 15.
- (41) Bensasson, R. V.; Land, E. J.; Truscott, T. G. *Flash Photolysis and Pulse Radiolysis*; Pergamon Press: Oxford, U.K., 1983.
- (42) (a) Palit, D. K.; Pal, H.; Mukherjee, T.; Mittal, J. P. *J. Chem. Soc., Faraday Trans.* **1990**, *86*, 3861. (b) Folm, S. R.; Barbara, P. F. *J. Phys. Chem.* **1985**, *89*, 4489. (c) Barbara, P. F.; Walsh, P. K.; Brus, L. E. *J. Phys. Chem.* **1989**, *93*, 29. (d) Avouris, P.; Gilbert, W. M.; El-Sayed, M. A. *Chem. Rev.* **1997**, *77*, 793.
- (43) Cohen, S. G.; Cohen, J. I. *J. Phys. Chem.* **1968**, *72*, 3782.
- (44) Singh, A. K.; Palit, D. K. To be communicated.
- (45) Leaver, I. H. *Tetrahedron Lett.* **1971**, 2333.